

Weak Fault Diagnosis of Metro Gearbox Based on Adaptive Variable Parameter SR and Underdetermined BSS

Yongliang BAI^{1,2}, JIANWEIYANG^{1,2}, Dechen YAO^{1,2}, Huijie WU^{1,2}

¹*School of Machine-electricity and Automobile Engineering, Beijing University of Civil Engineering and Architecture, Beijing, Beijing100044, China*

²*Beijing Key Laboratory of Performance Guarantee of Urban Rail Transit Vehicles, Beijing University of Civil Engineering and Architecture, Beijing, Beijing100044, China*

Abstract - With the research aim of weak fault diagnosis of metro gearbox, this paper proposed a new method that combines adaptive variable parameter Stochastic Resonance (SR) and under-determined Blind Source Separation (BSS). This method uses Artificial Fish Swarm Algorithm (AFSA) to optimize the parameters automatically in SR system, so the vibration signals with large parameters are transferred into signals with small parameters, then the method processes the signals with small parameters SR system to transfer energy of signals from high frequency to low frequency. Then the method uses Empirical Mode Decomposition (EMD) to enhance the dimension of single-channel signal so it can satisfy the requirements of BSS operation. Finally, the method uses Hilbert Transform (HT) to find the features to realize the weak fault diagnosis of metro gearbox.

Keywords - Adaptive Variable Parameter Stochastic Resonance; Underdetermined Blind Source Separation; Metro Gearbox; Weak Fault Diagnosis

I. INTRODUCTION

Metro gear box works in a harsh environment with changing conditions, its frequent start-stop produces dramatic changes to the load within short term and makes bearing structure prone to failure. Once the weak fault occurs, the fault of bearing will quickly expand to serious secondary fault and cause serious damage to the subway because the Metro gearbox bearing works at high level speed. So it is necessary for early diagnosis of weak fault in Metro gear box bearing to ensure the subway train running safety. The early fault signals of gear box bearing collected at the working scene contain many noises, the weak fault frequency stays in low frequency part where features of fault can easily be obliterated by these noises, and this phenomenon increases the difficulty of bearing weak fault feature extraction [1]. The methods of weak fault feature extraction is usually divided into two types: A. suppress or eliminate the noises in weak fault feature frequency part; B. strengthen weak fault features through nonlinear systems. Stochastic resonance is a kind of non-linear signal processing method, this method can transfer energy from noise to weak signals to enhance the energy of weak signals part [2]. Blind source separation is a kind of process that can recovery source signals without the knowledge of the mixing channel conditions or sources conditions but only need the statistical properties of the signals [3, 4]. The BSS has the ability to accurately distinguish weak components from the complex signals. Because of the special attributes of these two methods, it is able to decompose the sources of the signals after weak feature part was enhanced through the combination of SR and BSS and the completeness and accuracy of weak feature extraction can be assured.

Relevant studies have been made by many scholars, for example, He Huilong [5] studied the issue of ICA under strong noise mixing conditions, and he proposed a method that

use bistable SR system to reduce the time-domain noise, with his method, he improved the separation effect of noised ICA; and Shen Qinghua [6] proposed a two phase damage localization method based on nonlinear SR noise reduction and robust independent component analysis. With numerical examples, Shen proved that his method can achieve abnormal structural damage identification more accurate with lower SNR; and Zhao Jun[7] proposed a bearing fault diagnosis method based on Re-Scaling Cascaded Bistable SR and BSS; and Wang Jun[8] proposed an adaptive multi-scale noise induced SR method, his method can optimize parameters in large parameter SR adaptively.

However, all these existing researches lack the study on adaptive SR parameter optimization, so this paper proposes a method that combines adaptive variable parameter SR with underdetermined BSS, and the validity of this method is demonstrated by both simulation analysis and practical experiment.

II. ADAPTIVE VARIABLE PARAMETER SR AND UNDERDETERMINED BSS

A. Adaptive Variable Parameter SR

Only when the driving force, noise and nonlinear systems reach a state of equilibrium, the system can generate stochastic resonance phenomenon in a SR system. Scholars often use nonlinear bi-stable SR system to describe the stochastic resonance phenomenon. The SR system can be defined by the Articles of Lang, this equation can be described as a moving Brownian particle in a bi-stable potential well under the influence of noise and periodic driving force [9]:

$$\frac{dx}{dy} = -U'(x) + A_0 \sin(2\pi f_0 t + \varphi) + n(t) \quad (1)$$

Where, A_0 is periodic signal amplitude; f_0 is periodic signal frequency; φ is its phase; and $n(t)$ must satisfy the condition:

$$\begin{cases} n(t) = \sqrt[2]{2D}\xi(t) \\ E[n(t) * n(t + \tau)] = 2D\delta(t) \end{cases} \quad (2)$$

Where $\xi(t)$ is White Gaussian noise with 0 mean value and 1 variance; D is the noise intensity.

The bi-stable potential well $U(x)$ in (1) is defined by the following function:

$$U(x) = -\frac{a}{2}x^2 + \frac{b}{4}x^4 \quad (3)$$

Where, a and b are well parameters, they determine the barrier height of the system.

With the (1) and (3), we can calculate the output amplitude of this four order bistable potential well model with symmetrical reflection:

$$\bar{x}(D) = \frac{A_0 \langle x^2 \rangle_0}{D} \frac{r_k}{\sqrt{r_k^2 + \pi^2 f_0^2}} \quad (4)$$

Where, $r_k = \frac{1}{\sqrt{2\pi}} \exp(-\frac{\Delta U}{D})$ is Kramers rate, $\langle x^2 \rangle_0$ is system variance of smoothly without disrupting system (depending on $D, A_0 = 0$). Runge-Kutta method can be used to solve formula (1), thereby obtaining the numerical solution of differential equations. The key parameter in this method is step size h , this parameter determines the function error and calculation steps, a smaller h results a smaller function error and a larger calculation steps, so it is required to select an appropriate value of h to reduce the calculation steps with a normal function error.

The necessary condition of the formulas described above is adiabatic approximation; adiabatic approximation requires that f_0, A_0 and D in (1) must be less than 1. If any of these parameters is greater than 1, the stochastic resonance effect will not occur. The actual vibration signals barely satisfied this requirement, so it is necessary to transfer the actual signals with large parameters into a small parameter model. In the traditional process, researchers often choose a and b with empirical experience and the system does not have self-adaptability, so this paper uses Artificial Fish Swarm Algorithm (AFSA) to select optimized parameters. AFSA is a kind of swarm intelligence algorithm, this algorithm can simulate the simple underlying behavior of single artificial fish, and it can record and compare the feeding, clustering and rear-ending of fish group to achieve parameter optimization. The parameters to be optimized in this paper are a, b , and h , we assume that the current state of fish group is $P = [p_1, p_2, \dots, p_N]$, where N is artificial fish scale, and $p_i = [a, b]$ is the location of current artificial fish, this p_i represents the optimized parameters; and $Y = F(p_i)$ is food concentration at p_i , this Y also represents values of the objective function under condition of a, b, h . According to the calculation process, the artificial fish will be transferred to the position with high food concentration

by feeding, clustering and rear-ending behaviors. The place where contains the most of the artificial fish will be the best objective function, and the location of the place will be the optimal parameters [11].

AFSA needs an objective function as a guideline, this paper selects Signal-to-Noise Ratio (SNR) to be the objective function. SNR is a parameter that is defined as the ratio between signal power P_s and noise power P_N , it is often used to measure the power of input driving signal contained in output signals [12]. The output SNR of bistable stochastic resonance system under adiabatic conditions is:

$$SNR = \frac{\sqrt{2}a^2(\sqrt{b}A)^2 \exp\left(-\frac{a^2}{2bD}\right)}{4(bD)^2} \times \left\{ 1 - \frac{\frac{a^3(\sqrt{b}A)^2 \exp\left(-\frac{a^2}{2bD}\right)}{\left[\frac{\pi^2}{(bD)^2}\right]}}{\frac{2a^2 \exp\left(-\frac{a^2}{2bD}\right)}{\pi^2} + f_0^2} \right\}^{-1} \approx \frac{\sqrt{2}a^2(\sqrt{b}A)^2 \exp\left(-\frac{a^2}{2bD}\right)}{4(bD)^2} \quad (5)$$

We can optimize the parameters by locating the largest fish swarm when SNR reaches top. The optimization process of AFSA algorithm based on SNR can be described as:

1) AFSA needs to set the initial parameters of the algorithm, including the size of the fish scale N , the perception of artificial fish range V , the mobile step $Step$ of the fish, the crowding degree $Crow$, the maximum foraging number Try_number and the number of iterations M .

2) Algorithm needs to set objective function

$$Y = F(p_i) = SNR(a, b, h) \quad (6)$$

The initial state of the fish swarm can be defined by N fish randomly generated within the range of the parameters. Meanwhile the algorithm initializes the bulletin board for record of maximum objective function value Y_{best} and the position corresponding to the maximum objective function p_{best} .

3) For each artificial fish, the AFSA applies one clustering and rear-ending, and then the algorithm drives artificial fish to move to place with higher food concentration. In this process, independent artificial fish can find its own food too.

After all iteration operation, the AFSA replaces the contents in the bulletin with new parameter values obtained, and the algorithm calculates new SNR with these new parameters.

4) AFSA repeats the above steps for M times, and it uses the output of last iteration p_{best} as the optimal parameters.

The flow chart of AFSA algorithm is shown in figure 1.

The parameters a, b, h and signal S can be substituted into (1) after the parameters optimization in AFSA. We can use 4-order Runge-Kutta method to get the output signal $X(t)$ of adaptive variable parameters bi-stable SR system. With this process, we can transfer the energy of high-frequency part to low-frequency part and enhance the intensity of the weak signal, and we can get the energy-increased input signal that can be used in further BSS.

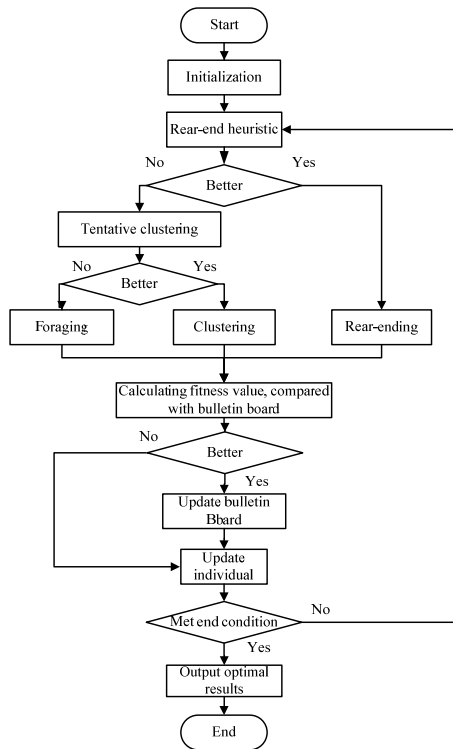


Figure 1. Flow chart of AFSA

B. Underdetermined BSS

The core idea of BSS is seeking a full rank separate matrix B , with this matrix, the output signal $\tilde{s}(t)$ can be the best estimate of source signal under the condition of unknown source S and unknown mixing matrix A [8]. BSS can be divided into linear BSS and nonlinear BSS because of different mixing ways, it also can be divided into instantaneous mixing and convolutional mixing. This paper focuses on the linear instantaneous mixed model.

The linear instantaneous mixture model of BSS is:

$$y(t) = As(t) + n(t) \tag{7}$$

Where, $y(t) = [y_1(t), y_2(t), \dots, y_M(t)]^T$ are M -dimensional observation signals obtained by sensors; and $s(t) = [s_1(t), s_2(t), \dots, s_N(t)]^T$ are N -dimensional unknown mutually statistical independent source signals; and A is a $M \times N$ dimensional mixing matrix. The process of solving linear instantaneous BSS is also a process of seeking a full rank $N \times M$ separate matrix W . After the separation of, we can get each source signal vector as much independent as possible. This process is shown in Figure 2.

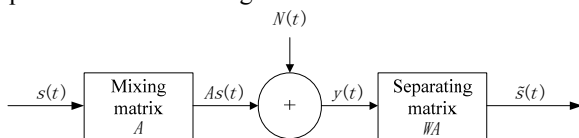


Figure 2. BSS model

The output signal in figure 2 is

$$\hat{s}(t) = W(As(t) + n(t)) = WAy(t) + Wn(t) \tag{8}$$

Formula (8) shows that if we want to get the estimated value of source signals (t) , we must make sure that the number of input signals are greater than the number of source signals N , this also means that the estimate matrix WA must be a full rank matrix. In metro gear box bearing vibration signals' acquisition, the number of signal channel are generally small while the number of sources are often numerous, this situation makes the corresponding separation matrix not reversible, it also become BSS into a pathological process which is often called underdetermined BSS. In order to solve the problem of insufficient input signal dimension in the underdetermined BSS, this paper introduces the Empirical Mode Decomposition (EMD) to enhance the dimension of single-channel signals.

EMD can decompose the signal into finite Intrinsic Mode Functions (IMFs) with different scales. These IMFs can express the interwoven internal messages completely because these IMFs are orthogonal to each other [13]. EMD can enhance the dimension of signals because of the IMFs. After the EMD on $X(t)$, we can obtain the IMFs from (t) , and these IMFs can be used to estimate the number of vibration source k . In order to estimate the number of sources, Bayesian information Criterion (BIC) [14] is introduced in this paper. BIC can analyze non-Gaussian signals, and this characteristic gives more reliability in the estimation. With BIC method, we can get the estimated number k , and then we can reassemble IMFs into k sets of new signals. Then we use BSS method based on Fast-ICA to separate k sets of IMF to get estimated signals $\hat{s}(t) = [\hat{s}_1(t), \hat{s}_2(t), \dots, \hat{s}_k(t)]$ [15], then the Hilbert Transform (HT) can be used to analyze the envelope spectrum of $\hat{s}(t)$ to find weak fault feature frequency in the spectrum figure to realize weak fault diagnosis.

The overall technical route in this paper is shown in figure 3.

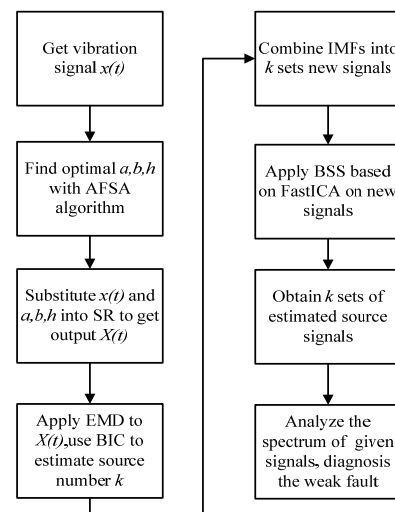
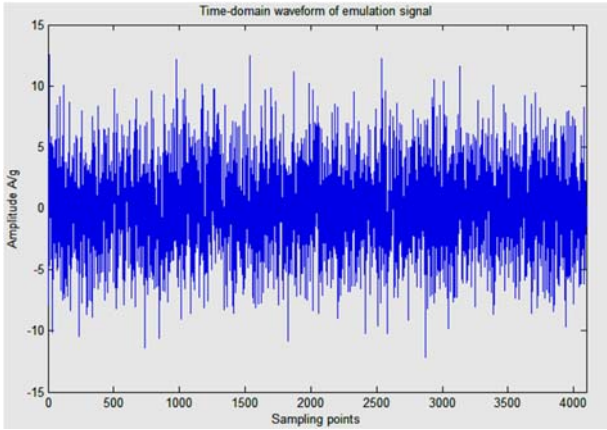


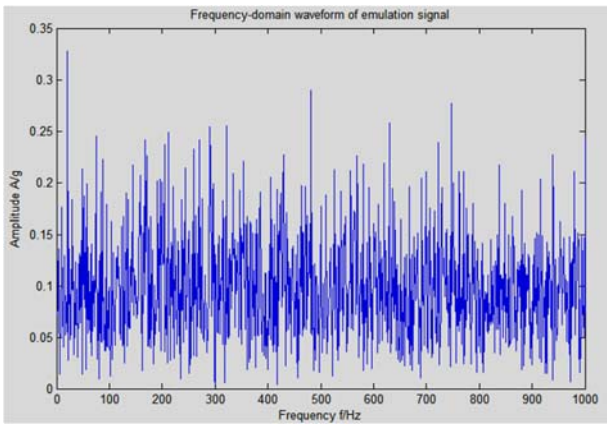
Figure 3. Overall technical route

III. EMULATION SIGNAL PROCESSING

In order to verify the validity of the method proposed in this paper, a simulated signal $x(t) = A_0 \sin(2\pi f_0 t + \varphi) + n(t)$ is constructed. Where $A_0 = 0.2, f_0 = 20\text{Hz}$; $n(t)$ is Gaussian white noise with variance $D = 3.1$, and the SNR of this signal is $SNR_x = 20\log_{10}\left(\frac{A}{\sqrt{2D}}\right) = -21.83\text{dB}$; The sampling frequency f_s is 4096Hz, the number of samples N is 4096. Both time-domain and frequency-domain signal wave forms are shown in Figure 4.



a) Time-domain waveform of emulation signal



b) Frequency-domain waveform of emulation signal

Figure 4. Time and frequency domain waveform of simulation signal

Figure 4 shows that we cannot find a clear cyclical component peaks in the time domain due to the strong influence of the noise, and we cannot find the peak of drive frequency in the frequency domain either.

We use AFSA to optimize the parameters of the simulation signals, and figure 5 shows the relationship between the objective function value and the number of iterations.

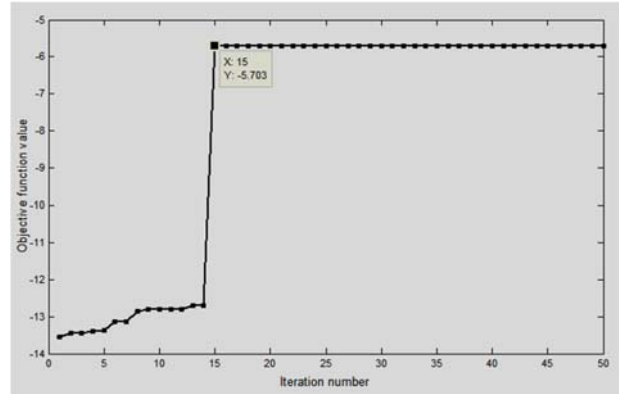
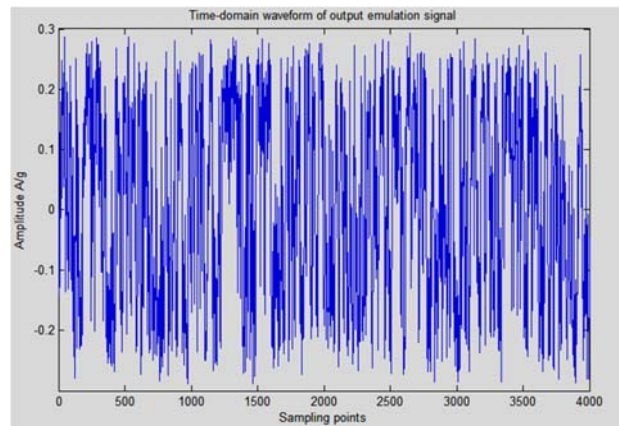
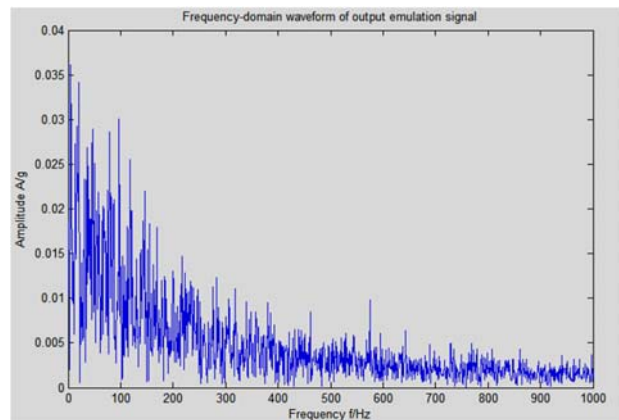


Figure 5. AFSA parameter optimization process

As we can see in figure 5, the algorithm converged after 15 iterations, and the results of optimization is $a = 0.01, b = 181, h = 0.006$. After we substitute this set of parameters and the emulation signal into SR system, we can get out put signals shown in Figure 6.



a) Time-domain waveform of output signal



b) Frequency-domain waveform of output signal

Figure 6. Output signal of SR emulation system

Figure 6 shows that after the energy transfer process of

SR system, the energy of low-frequency component in output signal has been significantly enhanced and the weak component of the signal has become prominent.

After we get the output of SR, we can decompose it with EMD, and the results of decomposition are 10 order IMFs, all the time-domain waveform of IMFs are shown in figure 7.

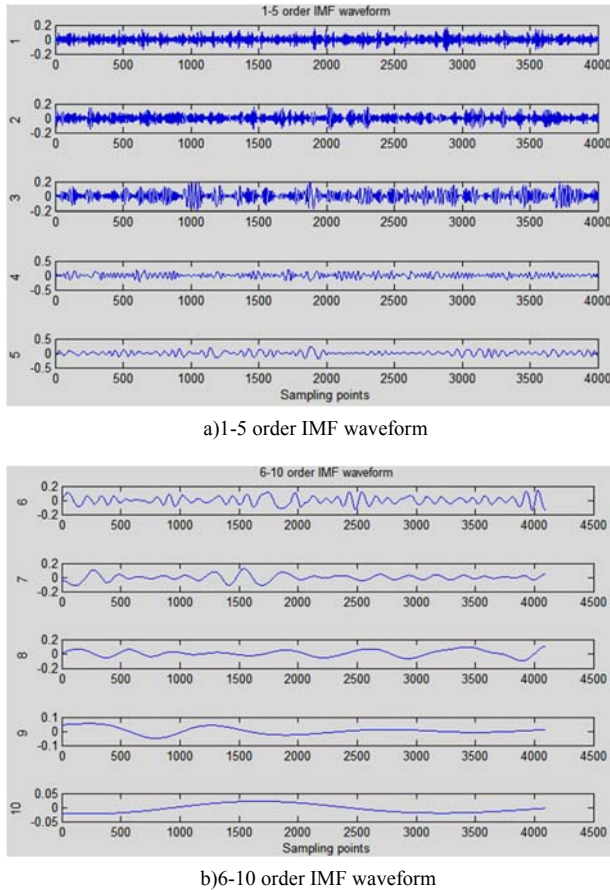


Figure 7. IMF time domain waveform of each order

We can estimate the sources number with BIC after we get IMFs. The calculate result shows that the BIC reaches the top when k is 3, so the estimated number of source is 3. Then we reassemble the IMFs into 3 groups and carry out determined BSS based on Fast-ICA on these 3 new signals, then we can get 3 output estimated signals $\hat{s}(t) = [\hat{s}_1(t), \hat{s}_2(t), \hat{s}_3(t)]$, with these output signals, we can carry out HT to find the envelope of signals. The results of HT are shown in figure 8.

We can find the peak of 21Hz clearly in figure 8, with the consideration of tolerance error, we can equal this feature with drive frequency in emulation signal, and thus we realized the diagnosis of weak fault signals.

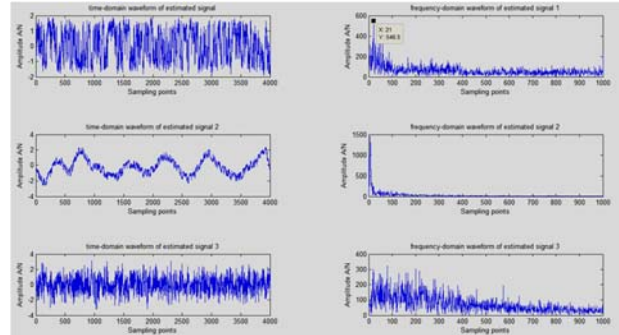


Figure 8. Time - frequency spectrum of the estimated signal

IV. MEASURED SIGNAL PROCESSING

In order to verify the effectiveness of the method proposed in this paper, we collect actual vibration data from metro gear box test rig. The experimental rig used in this paper is produced by SpectraQuest, the experimental rig can achieve different transmission ratio with different assembled ways. This test rig can simulate various failure modes and it can provide reliable experimental data for this paper. The parameters of the test rig are shown in Table I.

TABLE I. PARAMETERS IN TEST RIG

Transponder of input shaft	Drive ratio	Type of bearing
10Hz	19:100	NU 202 ECP (Cylindrical Roller Bearings)
Bearing pitch diameter	Rolling diameter	The number of rolling body
24.8mm	5.5mm	11

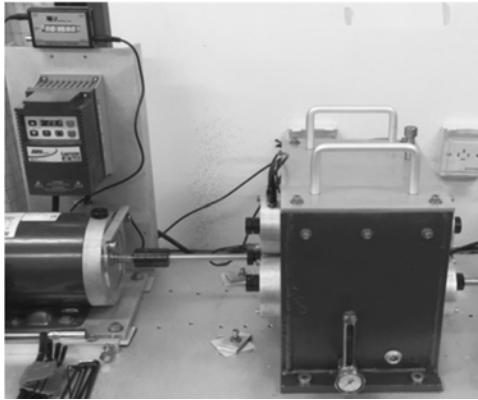
In this paper, we preset inner ring fault on the bearing. The contact between rotational part and fault will generate periodic impact signals. The frequency of this impact is related to bearing structure and rotational speed. The fault frequencies corresponding to cylindrical roller bearing is:

$$\begin{cases} F_{\text{Bearing inner ring}} = \frac{n}{2} f_r \left(1 + \frac{d}{D}\right) \\ F_{\text{Bearing outer ring}} = \frac{n}{2} f_r \left(1 - \frac{d}{D}\right) \\ F_{\text{Bearing rolling elements}} = \frac{n}{2} f_r \left(1 + \left(\frac{d}{D}\right)^2\right) \end{cases} \quad (9)$$

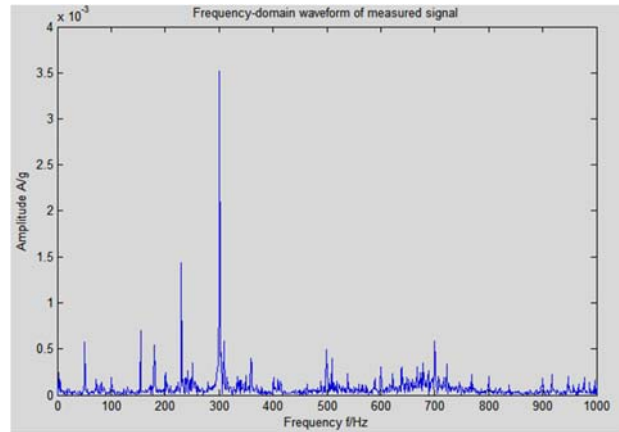
Where, Z is gear ratio; n is number of rolling elements; f_r is rotational frequency of input shaft; d is roller diameter; D is bearing pitch.

After the calculation of characteristic frequency according to (9), we can know that $F_{\text{Bearing inner ring}}$ is 67.19Hz, $F_{\text{Bearing outer ring}}$ is 42.8Hz and $F_{\text{Bearing rolling elements}}$ is 23.65Hz.

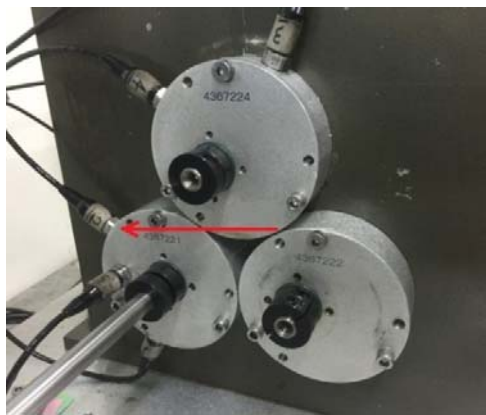
The rig and sensors used in this paper is shown in Figure 9. The acceleration sensors are arranged on the end cover of the bearing seat. In this experiment, the sampling frequency is 20KHz, the sampling time is 5S and the input shaft frequency is 10Hz.



a) Metro gear box failure test rig



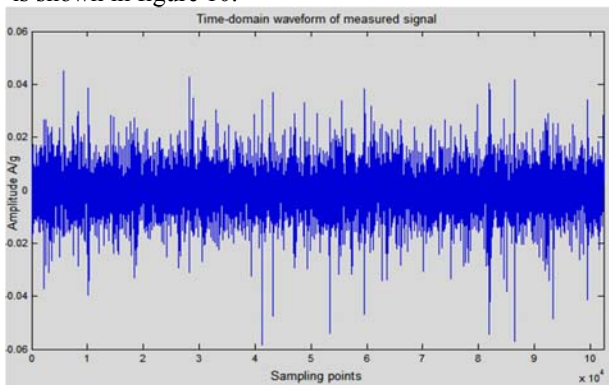
b) Frequency-domain waveform



b) Sensors and measuring point

Figure 9. Test bench and sensors

The single-channel vibration data is collected by the sensor shown in Figure 9. Its time-frequency domain waveform is shown in figure 10.



a) Time-domain waveform

Figure 10. Waveform of measured signal

As we can see in figure 10, there are no components that corresponding to fault feature frequency both in time-domain and frequency-domain.

After we use AFSA to optimize the parameters of the signal, we can get the relationship between the objective function value and the iteration number; the result is shown in figure 11.

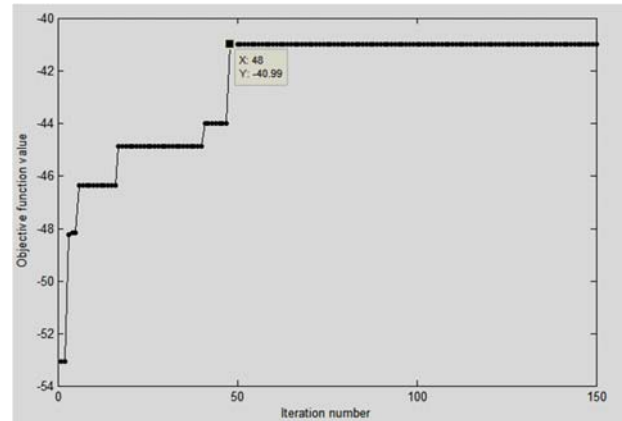
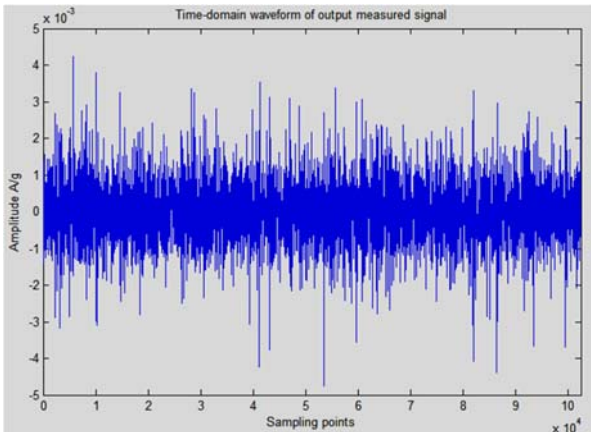
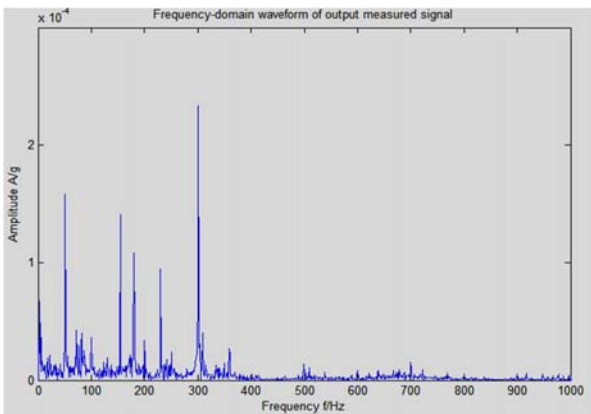


Figure 11. AFSA parameter optimization process

Figure 11 show that the algorithm obtains optimal target parameters after 48 iterations. In this case, the corresponding parameters are $a = 3.76$, $b = 55.82$, $h = 0.02$. After we substitute the obtained parameters and original signals to SR system, we can get the output signals shown in Figure 12.



a)Time-domain waveform of output measured signal

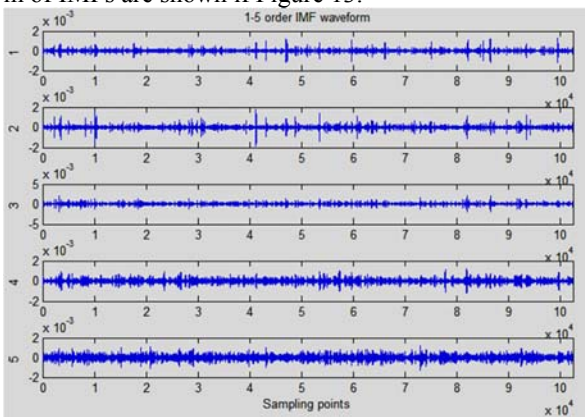


b)Frequency-domain waveform of output measured signal

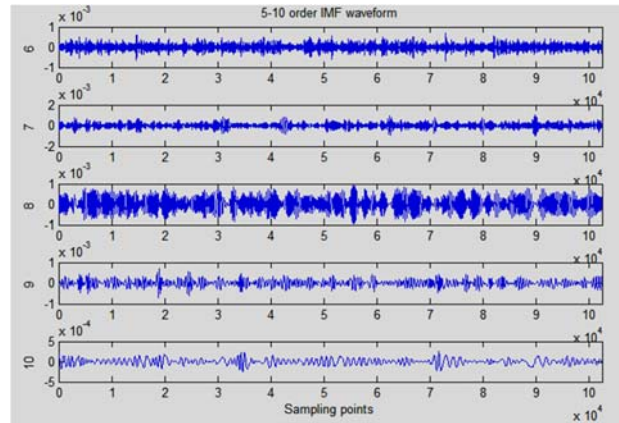
Figure 12.Output of measured signal

As we can see in figure 12, the energy signals in low frequency has been enhanced clearly compared to figure 10, this phenomenon proves the efficiency of the energy transfer characteristics of SR.

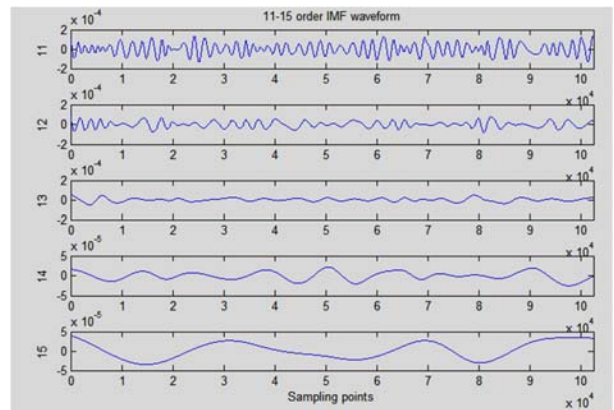
Then we carry out EMD on the output signal of SR system and we can get 15 order IMFs, the time-domain waveform of IMFs are shown in Figure 13.



a)1-5 order IMF waveform



b)6-10 order IMF waveform



b)11-15 order IMF waveform

Figure 13.Time domain waveform of each order IMF

We use BIC to estimate the number of source signals in IMFs, and we get maximum BIC when k is 2, this proved that the signal has 2 estimated sources. Then we combine these 2 IMFs into 2 new sets of signals and use these 2 new signals as the input 1 of BSS. After we carry out the BSS process based on Fast ICA, we can get 2 groups of estimated source signals. Then we use HT to analyze the signals, the results are shown in figure 14.

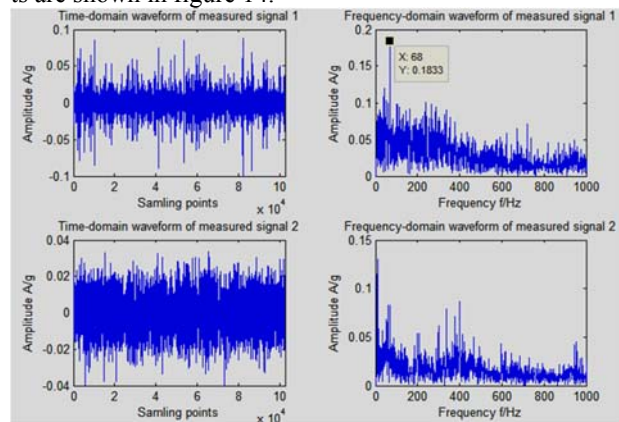


Figure 14.Time-frequency spectrum of measured signal

Figure 14 shows the presence of peak 68Hz, this peak matches the preset fault feature frequency well, and namely, we realized the diagnosis of weak fault in metro gear box successfully.

V. CONCLUSIONS

In conclusion, the method proposed in this paper has the ability to select parameter a , b and h in bi-stable SR adaptively. And these processes also guarantee the large parameter SR process can consist with the principle of adiabatic condition. With this method, we can enhance the energy of weak components in signals clearly, and then we can separate source signals of energy-enhanced output signal of SR system through Undetermined BSS. With this method, we can realize weak fault diagnosis in Metro gear box.

Both emulation signals and measured signals are applied to the proposed method, and the results indicate that this method can find corresponding fault characteristic frequency to each fault successfully. With both theoretic analyses and testing results, it is proved that this method can be used as a new idea of weak fault diagnosis in metro gear box.

ACKNOWLEDGMENT

The authors acknowledge the financial support from the Great-Scholars-Program (CIT & TCD20150312) and Natural Science Foundation of China (51175028).

REFERENCES

- [1] TANG Xianguang, Application of Rolling Element Bearing Envelope Analysis Based on Short Time Fourier Transform and Independent Components Analysis[J], *Journal of Mechanical Strength*, 34(1):1-5, 2012.
- [2] HE Q, Wang J, Effects of multiscale noise tuning in stochastic resonance of weak signal detection[J], *Digital Signal Processing*, 22(4):614-621, 2012.
- [3] ROAN M J, ERLING J G, SIBUL L H, A new, nonlinear, adaptive, blind source separation approach to gear tooth failure detection and analysis[J], *Mechanical Systems and Signal Processing*, 16(5):19-740, 2002.
- [4] Haykin Unsupervised Adaptive Filtering Volume, Blind source separation, New York, Wiley, Chi Chester, 2000.
- [5] HEHui-long, Noisy ICA Based on Cascaded Bistable Stochastic Resonance Denoising[J], *Journal of Tianjin University*, 12:1517-1520, 2006.
- [6] SHEN Qing-hua, Two-stage damage localization method by integrating stochastic resonance theory and Robust ICA Algorithm[J], *Journal of Fuzhou University*, 6:917-918, 2014.
- [7] ZHAO Jun, Bearing Fault Diagnosis Based on Stochastic Resonance and BSS/ICA[J], *JOURNAL OF BEIJING UNIVERSITY OF TECHNOLOGY*, 2:177-179, 2014.
- [8] Jun Wang, Methodology of Fault Diagnosis of Rotating Machinery via Multiscale and Nonlinear Condition Feature Enhancement[J], *University of Science and Technology of China*, China, 2015.
- [9] Benzi R, Sutera A, Vulpiani A, The mechanism of stochastic resonance[J], *Journal of Physics A: Mathematical and General*, 14(11):453-457, 1981.
- [10] Gammaitoni L, Hanggi P, Jung P, et al, Stochastic resonance[J], *Reviews of Modern Physics*, 70(1):223-287, 1998.
- [11] Shen W, Guo X, Wu C, et al, Forecasting stock indices using radial basis function neural networks optimized by artificial fish swarm algorithm[J], *Knowledge-Based Systems*, 24(3):378-385, 2011.
- [12] ZHU Guangqi, Experimental research of weak signal detection based on the stochastic resonance of nonlinear system[J], *Aicaphysica sinica*, 5:3002-3006, 2010.
- [13] HUANG NE, SHENZ, LONGSR, The empirical mode composition and the Hilbert spectrum for nonlinear random-stationary time series analysis[J], *Proceedings of the Royal Society of London, Series A: Mathematical, Physical and Engineering Sciences*, 454(1971):903-995, 1998.
- [14] DING Q, KAY S, Inconsistency of the MDL: on the performance of model order selection criteria with increasing signal-to-noise ratio[J], *IEEE Transactions on Signal Processing*, 59(5):1959-1969, 2011.
- [15] Stone JV, Blind source separation using temporal predictability[J], *Neural Computation*, 7:150-165, 2001.
- [16] Zhong Youming, Study on a New Transform Method for Vibration Signal[J], *Journal of Vibration Engineering*, 15(2):234-236, 2002.